

Original research article

Enhancing the bone healing on electrical stimuli through the dental implant

Running title: Bone healing on electrical stimuli

Letícia Bins-Ely¹, Daniela Suzuki², Ricardo Magini¹, Cesar A. M. Benfatti¹, Wim Teughels³, Bruno Henriques^{4,5}, Júlio C. M. Souza*^{5,6}

¹Post-graduate Program in dentistry (PPGO), School of Dentistry (ODT), Universidade Federal de Santa Catarina (UFSC), 88040-900, Florianópolis, Santa Catarina, Brazil.

²Institute of Biomedical Engineering, Universidade Federal de Santa Catarina (UFSC), 88040-900, Florianópolis, Santa Catarina, Brazil.

³Department of Oral Health Sciences, University Hospitals Leuven, Katholieke Universiteit Leuven, Leuven, 3000, Belgium

⁴Dept. of Materials Engineering, Universidade Federal de Santa Catarina (UFSC), 88040-900, Florianópolis, Santa Catarina, Brazil.

⁵Center Microelectromechanical Systems (CMEMS), Dept. Mechanical Engineering (DEM), University of Minho, Guimarães, 4800-058 Portugal.

⁶Department of Dental Sciences, University Institute of Health Sciences (IUCS), CESPU, Gandra PRD, Portugal

***Corresponding author:**

Júlio C M Souza, PhD, DDS, MSc Email: jsouza@dem.uminho.pt;

Center Microelectromechanical Systems (CMEMS)

Dept. Mechanical Engineering (DEM),

University of Minho, Portugal.

Phone: +351 963643905

orcid.org/0000-0001-7999-4009

Conflict of Interest Statement:

No conflict of interest

Author contribution statement:

Data collection/ analysis/interpretation: Letícia Bins Ely, Júlio Souza, Daniela Suzuki

Drafting article: Letícia Bins-Ely, Cesar Benfatti, Júlio Souza

Concept/design/Critical revision of the article: Bruno Henriques, João Caramês, Wim Teughels, Júlio Souza

Approval of article: Bruno Henriques, Daniela Suzuki, Júlio Souza

Statistics, Funding secured by: Bruno Henriques, Wim Teughels, Cesar Benfatti

Abstract

Purpose: The aim of this study was to evaluate the influence of different density and amplitude of electric current on the percentage of bone-implant contact (BIC) formation using the finite element method.

Materials and Methods: Numerical models were performed on commercially pure titanium grade IV implants connected to a 1.5 V battery with an electrical resistance (R) at 150 k Ω on 10 μ A or at 75 k Ω on 20 μ A. The percentage of simulated BIC was analysed by varying the electric current from 1 up to 60 μ A. The variation of electric current application was simulated for coronal and apical peri-implant regions.

Results: The findings showed that a direct and constant electric current source below 10 μ A does not provide a proper current density for osseointegration (BIC < 55%). Electric current sources ranging from 10 to 20 μ A resulted in an increase in BIC above 60% while BIC reached 90% on 30 to 40 μ A. Also, the application of the current source on 20 μ A at the apical peri-implant region resulted in the highest BIC percentage at around 86.1%.

Conclusions: The location and intensity of the electrical current source can increase the resultant electrical current density at the implant-bone and enhance the bone healing process. Although the model is a simplified version of the biological process in the bone-implant interface, the findings obtained in this study can predict a magnitude of electrical current density required to stimulate osseointegration.

1. Introduction

Since the 1970s, titanium-based implants have been widely used in dentistry due to their physicochemical and biological behavior to establish a direct contact with the surrounding bone ¹. Conventional loading - at least three months in the mandible and six months in the maxilla ² it has been recommended to minimize the risk of soft tissue encapsulation, consequent loss of osseointegration and implant failure ^{1,3}. Although 10-year implant survival rate of 99.7% ⁴, recent studies have pursued to decrease the bone healing period ⁵. In fact, peculiar clinical conditions can occur such as the placement of implants in regions with poor bone quality and volume ⁶. Also, bone grafts and bio-absorbable membranes are often required for vertical and horizontal bone augmentation ⁷. Factors related to the patients, prosthetic, and surgical conditions statistically affect implant failure rates. Thus, shorten the healing time can avoid early risks of failures in implant-supported rehabilitation ⁸.

Changes in morphological aspects and chemical composition of implant surfaces affect the dynamics of bone healing at bone-implant contact area during the initial stages after implant placement ⁹. Several studies demonstrated that rough titanium surfaces induce the activation of platelets to release growth factors ^{10,11}, improves osteogenesis ¹², affects the degree of osseointegration ¹³, and enhances mechanical stability ¹⁴. Additionally, surface energy affects the biological response to the implant that speeds up the early stages of cell adhesion, proliferation, differentiation and bone mineralization. Thus, wettability probably determines the adsorption of proteins onto the surface and the formation of a blood clot and a fibrin network ¹⁵. Nowadays, a combination of physical and chemical modification of implant surfaces is the most

common method used for implant surface. Among them, grit-blasting with abrasive particles followed by etching (SLA method) is used for several implant manufacturers. Clinical studies showed 5-year cumulative success rate above 96%^{16–18} and a robust bone-implant contact (BIC), ranging from 67 to 81% on implants treated by grit-blasting and etching¹⁹. Recent methods deal with electrochemical procedures for biomimetic functionalization of dental implants. Functionalization by using bioactive ceramics aims to mimic the natural deposition of calcium phosphate apatite crystals on the implant surfaces leading to the precipitation of biological apatite on the surface of the implant^{20,21}.

Electrical stimulation of the bone after implant placement has been studied in the last years^{22,23}. An invasive electrochemical method, and most commonly used, is the direct current (DC) stimulus, approved by the Food and Drug Administration (FDA) in 1979. DC stimulus consists of a battery that generates an electric field (EF) to growing cells, either directly through the implant device or indirectly through the medium where they are growing²⁴ and has been used clinically for over 36 years thenceforth for fracture healing²⁵. On the other hand, non-invasive approaches for bone growth stimulation namely inductive stimulus (EI) has been reported in literature. EI generates capacitive stimulus (EC) and an electromagnetic field from coils connected in series through external electrodes²⁶. In fact, electric stimulus speeds up bone formation process, probably stimulating the migration of pre-existing osteoblasts and mesenchymal cells to the implant-bone interface during the first stage of the osseointegration process. Despite several experimental *in vitro* and *in vivo* studies^{22,23,27–32}, the underlying mechanism by which electrically induced osteogenesis occurs remains unclear. There is no consensus in the literature regarding the operating

principles of both electric current densities $0.01 \text{ A/m}^2 < J < 0.5 \text{ A/m}^2$ ²⁴ and amplitudes $7 \text{ } \mu\text{A}$ to $50 \text{ } \mu\text{A}$ ²⁵ applied in the bone-dental implant interface. However, titanium implants submitted to $20 \text{ } \mu\text{A}$ electrical current application for 14 days showed better bone apposition on the implant surface with 82% BIC ($p < 0.01$) ²³. This result shows the positive correlation between the percentage of bone-implant contact and the application of electric current of $20 \text{ } \mu\text{A}$ ²³. To our knowledge, experimental studies have not involved different clinical situations linked to the implant design, electrical source site, and the bone conditions.

Considering several factors that affect the osseointegration process, finite element analyses can also be a good strategy to preliminary distinguish key aspects to enhance osseointegration of implants. In this way, different parameters are separately evaluated leading to a proper planning of *in vitro* and *in vivo* studies. Thus, the aim of this study was to evaluate the influence of different density and amplitude of electric current on the percentage of bone-implant contact using the finite element method. The null hypothesis of this study was that the ideal electrical current application is around $20 \text{ } \mu\text{A}$ and that the position of the current source inside the implant influences the BIC area.

2. Material and methods

2.1. Numerical model of the implant-battery-bone assembly

The numerical model used in the present study was designed from the histomorphometric evaluation of the bone implant contact after *in vivo* electrical stimulation of dental implants. ²³ Therefore, that represented an experimental electrical stimulation for 15 days. Commercially pure titanium (cp Ti) grade IV implants

were connected to a 1.5 V battery with an electrical resistance (R) at 150 k Ω on 10 μ A or at 75 k Ω on 20 μ A. The average current density for 10 μ A at body/apex peri-implant region is 66mA/m², and at cervical region is 175mA/m² and for 20 μ A at body/apex peri-implant region is 132mA/m² and at cervical region is 350mA/ m². The positioning of the electrical resistance (h) affected the electrical current flow (I) as shown in Figure 1. 1. Electric current travelled a shorter path when the electrical resistance was positioned closer to the battery (cervical portion). The electrical current did not flow through the apical regions (Figure 1B).

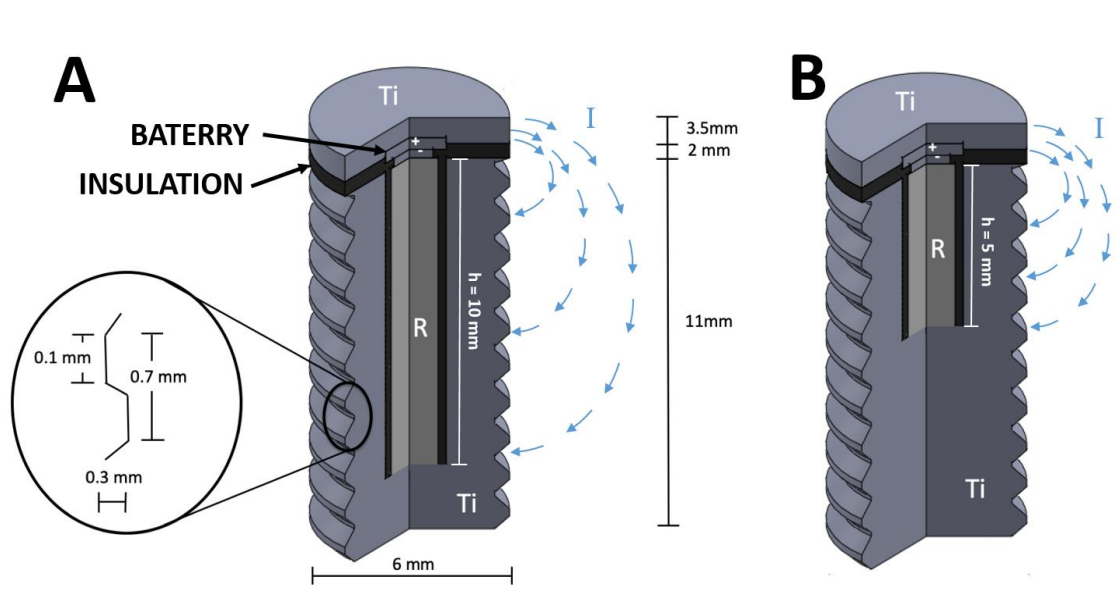


Figure 1. Schematic illustration of the implant-battery assembly. Ti represented the titanium implant while R corresponded to the electrical resistance. Cross-sectioned drawing reveals the internal design of the implant coupled to the battery. Arrows indicate differences in electric current flow (I) depending on the positioning of the electrical resistance to (A): $h=10$ mm and (B) $h=5$ mm.

The geometric details on the implant and battery can also be seen in Figure 2. The dielectric properties of the materials involved in the implant-battery-bone set up are described in Table 1.

Table 1 – Dielectric properties of materials and tissues involved in the study.

| Material | Electric conductivity σ (S/m) | Relative permittivity ϵ_r | Ref. |
|--------------------|---|---------------------------------------|-------|
| Cp Ti grade IV | 2.5×10^6 | 1.6×10^2 | 33 |
| Blood clot | 1.7×10^{-3} | - | 34 |
| Insulating (nylon) | 1×10^{-12} | 8 | 35 |
| Cancellous bone | 2×10^{-1} | 1×10^3 | 36 |
| Cortical bone | 2×10^{-2} | 5×10^2 | 36,37 |
| Soft tissue | 4×10^{-2} | 6×10^4 | 37,38 |

Details of the implant to bone interface are shown in Figure 2A. The representative section of the implant-bone region was selected according to previous studies considering a cancellous bone with 21 mm in height ³⁶, cortical bone with 1 mm in height ^{36,37} soft tissue with 2 mm in thickness ^{37,38}, and blood clot with 0.3-0.6 mm in thickness ³⁴. The positioning of the implant in length, depth, diameter, and surrounding bone volume were proper to validate the effect of the electrical stimuli on the bone healing in maxilla and mandibulae bone as shown in the referred previous in vivo study.

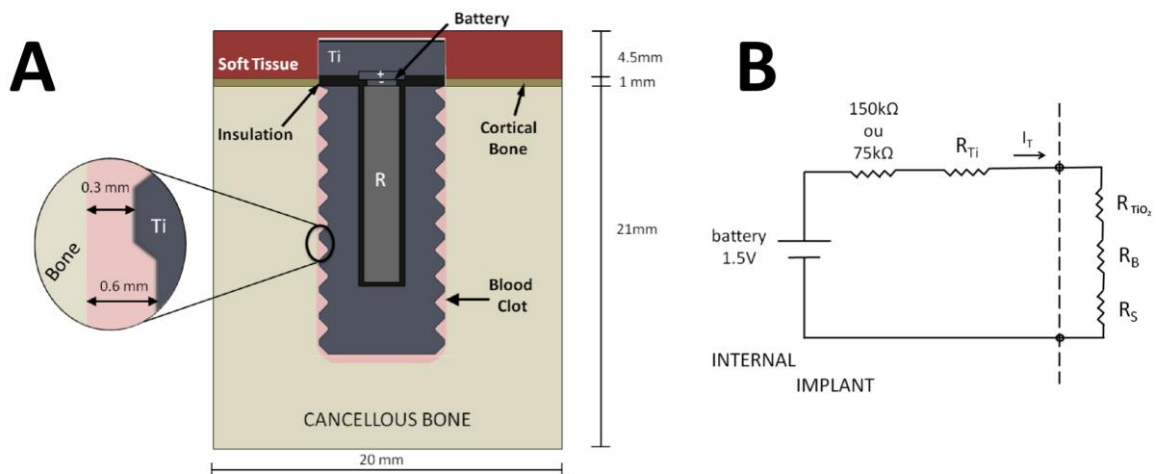


Figure 2. Schematics of the implant and batter surrounded by the peri-implant tissues. (A) The implant to bone region is shown in details according to previous studies ³⁴. (B) Equivalent electric circuit of the dental implant and surrounding tissues.

The equivalent electric circuit related to the implant-battery and peri-implant tissues is shown in Figure 2B, where R_{Ti} is the electrical resistance for cp Ti while R_{TiO_2} is the electrical resistance for TiO_2 and blood clot; R_B is the electrical resistance for the cancellous and cortical bone and R_s is the electrical resistance for soft tissue. The total electrical current flowing on the dental implant and surrounding tissues is represented by I_T (Fig. 2B).

2.2. Finite element analysis

Three-dimensional (3D) model calculations were run on a personal computer (Intel Core i5-2500, 3.3 GHz, 4 GB RAM) with Windows 7 (x64; Microsoft, Inc., Redmond, WA, USA) operating system. The electric field distribution on the implant-battery assembly and peri-implant tissues was computed by finite element method (FEM) using the COMSOL Multiphysics® (Stockholm, Sweden). A grid independence study was performed to establish an optimized mesh. This numerical model generated 96,185 tetrahedral elements by FEM. The local electric field (E) value at each one of the tetrahedral elements calculating dominion was determined by a steady current module (AC/DC module) following the Laplace equation as follow:

$$-\nabla \cdot (\sigma \nabla \cdot V) = 0 \quad (1)$$

where σ is the tissue conductivity (S/m) that is dependent on the electric field and V is the electric potential. Neumann's boundary condition was applied for external insulate surfaces while interface between different materials were assessed by Dirichlet's boundary condition ³⁹.

2.3. Parameters models

Current computational limitations do not allow simultaneously simulating dimensions of titanium oxide thickness (nanometres) and implant dimensions (millimetres). To work around this dimensional difference of more than 100,000 times, the titanium oxide and clot were considered to be a single macroscopic system with specific electrical characteristics. These electrical characteristics were obtained by matching the electrical conductivity of the medium with the experimental results obtained by Bins-Ely et al (2017) ²³. The electrical conductivity (σ_{BC+TiO_2}) of the implant to bone region was simulated from 0.05 to 0.5 S/m. The relative permittivity was considered similar to that recorded for the blood (4×10^3 ⁴⁰). The experimental and simulated bone-implant region ²³ were compared to those of dental implants with resistance at 150 k Ω and 75 k Ω . The electrical current was applied at about 10 μ A for 150 k Ω or 20 μ A for 75 k Ω . Then, the percentage of simulated bone-implant region was analysed within an electric current ranging from 1 up to 60 μ A and $\sigma_{BC+TiO_2} = 0.30$ S/m. The variation of electric current application was simulated for cervical (h=5 mm) and apical peri-implant region (h=10 mm). The ideal electrical current density for osseointegration $0.01 \text{ A/m}^2 < J < 0.5 \text{ A/m}^2$ was illustrated by coloured images. A low current density for osseointegration ($J < 0.01 \text{ A/m}^2$) was represented in black colour while high current density ($J > 0.5 \text{ A/m}^2$) to induce tissue necrosis was suggested in white colour ²⁴.

3. Results

The initial evaluation of the electric current source on the implant simulation revealed an electrical current intensity at 10.5 μ A for 150 k Ω and 21.1 μ A for 75 k Ω .

Electrical conductivity of the implant-bone gap region filled by blood clot was below 0.45 S/m on an electric current source at 21.1 μA . The bi-dimensional reconstruction of the model by finite element modelling is shown in Figure 3.

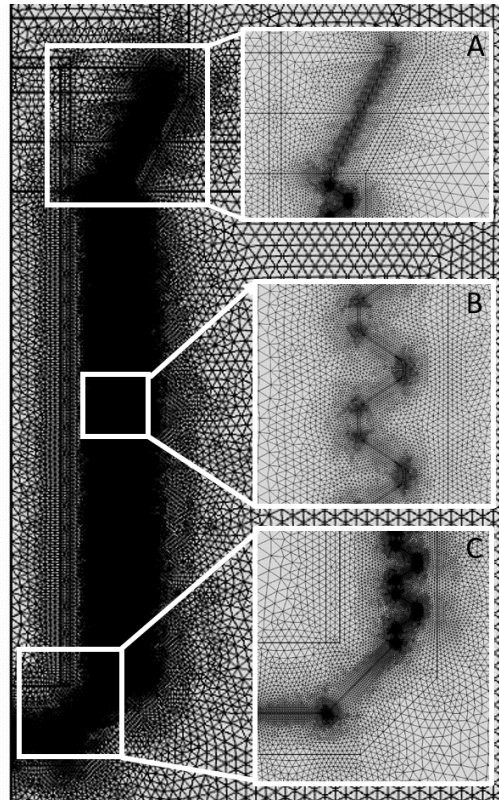


Figure 3. 2D axisymmetric finite model of implant with surrounding tissues. The white square regions reveal details of implant geometry by finite element modelling: (A) Crest module, (B) body with V-Thread, and (C) apex.

In the computational simulation, $\sigma_{\text{BC+TiO}_2}$ variation ranged from 0.05 up to 0.5 S/m that was acceptable for the current source of 20 μA . Percentage of BIC (%) within the electrical conductivity ($\sigma_{\text{BC+TiO}_2}$) ranging from 0.05 up to 0.2 S/m for 10 μA is shown in Figure 4.

Results revealed a threshold value for osseointegration at 0.35 S/m that means an electrical conductivity ($\sigma_{\text{BC+TiO}_2}$) value for a minimum osteogenic stimulation (Figure 4).

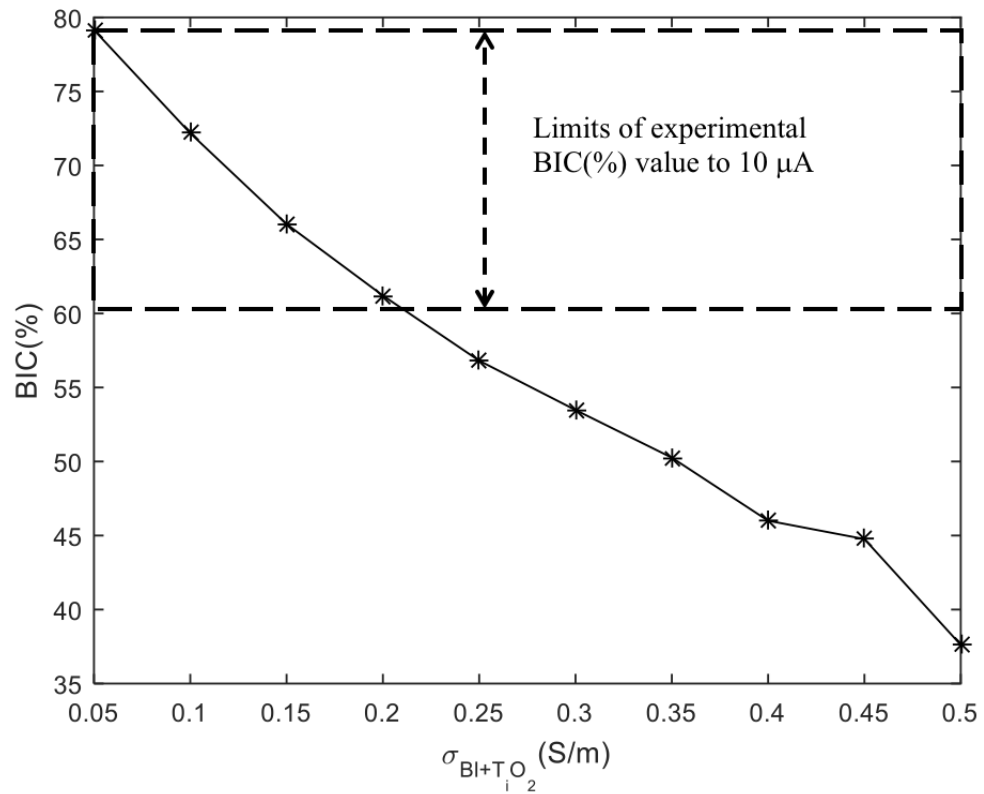


Figure 4. Electrical conductivity of the bone-implant contact (BIC) region. The arrow delimits the experimental variations of BIC (%) results for 10 μA obtained by a previous in vivo study ²³.

The current density distribution (J) though the implant on $\sigma_{\text{BC+TiO}_2} = 0.3 \text{ S/m}$ is shown in Figure 5.

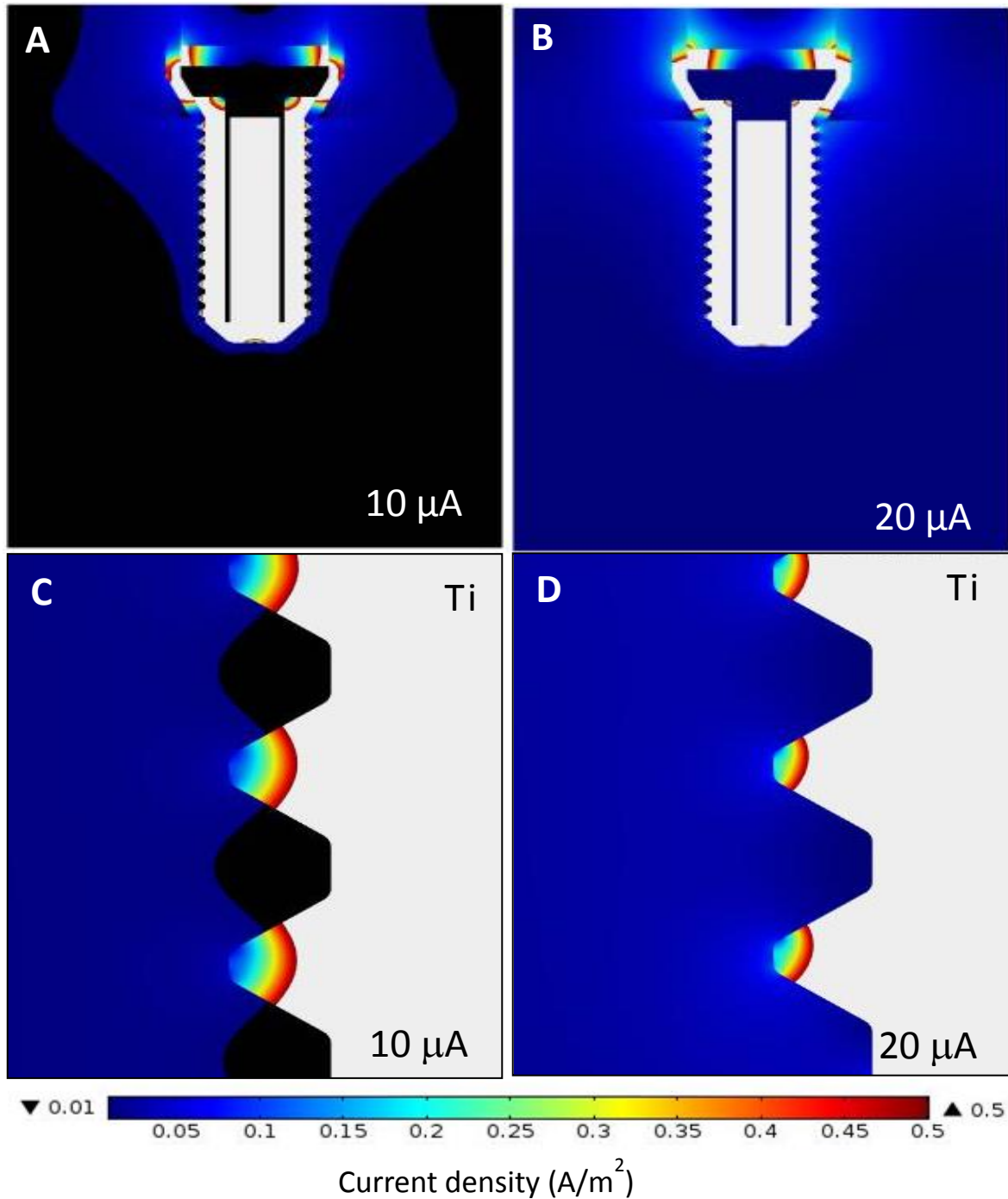


Figure 5. Distribution of current density on implant for (A,C) 10 μA or (B,D) 20 μA . $\sigma_{\text{BC}+\text{TiO}_2}=0.3 \text{ S/m}$. (C,D) The bone-implant interface shown in details. Black colour indicated $J < 0.01 \text{ A/m}^2$ while rainbow colour was at $0.01 \text{ A/m}^2 < J < 0.5 \text{ A/m}^2$, and white at $J > 0.5 \text{ A/m}^2$.

Such high conductivity value generates low resistance values, which brings the worst hypothesis for the study, underestimating the osseointegration area. The total electric current applied to the implant at 10 μA (A,C) or 20 μA (B,D) is shown in Figure 5.

The influence of electrical current sources on the bone-implant contact (BIC) percentage is shown in Figure 6 and 7. Electrical conductivity ($\sigma_{\text{BC+TiO}_2}$) was at 0.3 S/m for both analyses. In Figure 6, electrical current stimulation was performed at the apical peri-implant region ($h = 10$ mm) and showed a BIC of around 80% on 20 μA , 93% on 30 μA ; and 98% on 40 μA . In Figure 7, electrical current stimulation was performed at the cervical peri-implant region ($h = 5$ mm) and showed lower BIC (%) values for all current sources.

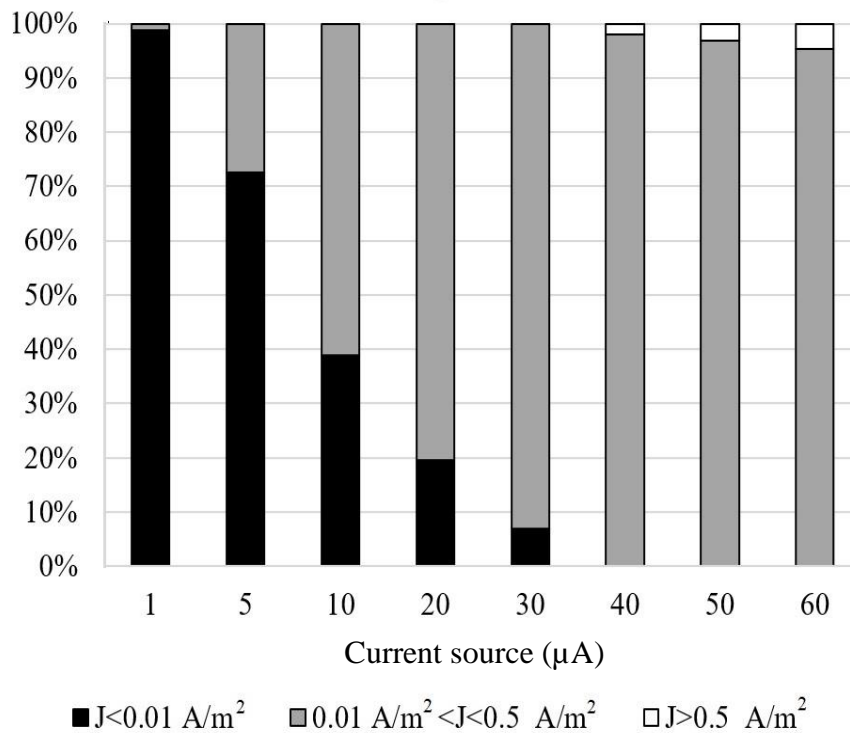


Figure 6. Influence of the current source variation on the bone-implant contact (BIC) percentage. $\sigma_{\text{BC+TiO}_2}=0.3 \text{ S/m}$. $h = 10$ mm, current applied at the apical peri-implant region.

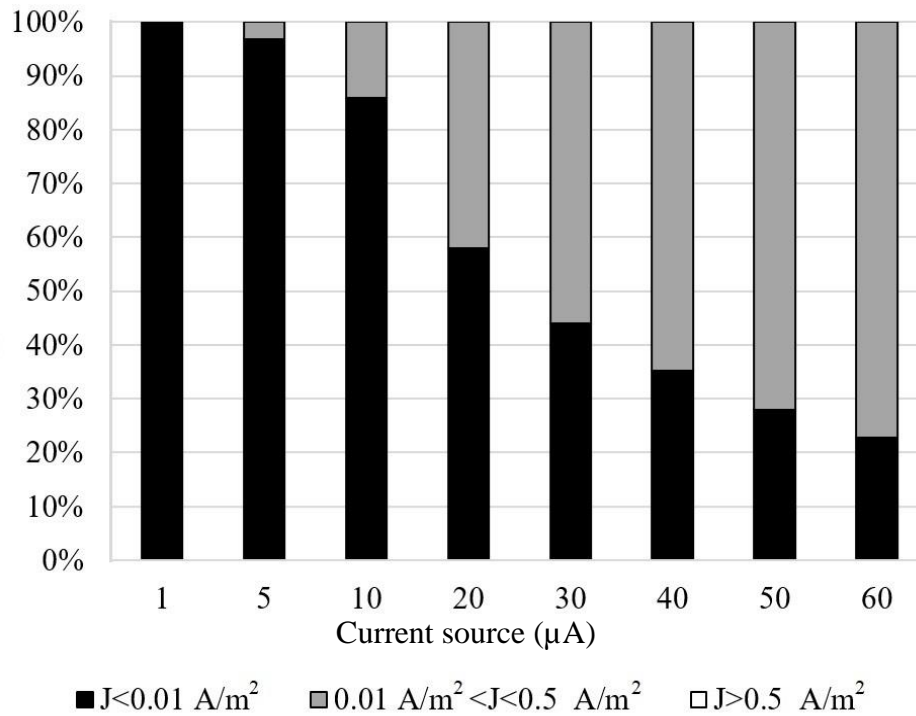


Figure 7. Influence of the current source variation on the bone-implant contact (BIC) percentage. $\sigma_{\text{BC}+\text{TiO}_2}=0.3 \text{ S/m}$. $h = 5 \text{ mm}$, current applied in the cervical peri-implant region.

4. Discussion

The results of the present study support the rejection of the null hypothesis. They showed that a source applying a direct and constant electric current below $10 \mu\text{A}$ does not evidence acceptable current density values required for osseointegration ($\text{BIC} < 55\%$). However, current sources ranging from 10 up to $20 \mu\text{A}$ promoted BIC values above 60% while sources from 30 up to $40 \mu\text{A}$ resulted in BIC values above 90% . In the case of implant geometry, the application of the current source at the apical peri-implant region (closer to the implant apex) resulted in BIC values at 86.1% .

In this study, the electrical conductivity of the titanium oxide and blood clot was estimated at 0.3 S/m (Fig. 4) considering there is a chemical reaction between the TiO_2 -film and blood that changes their chemical composition, thickness, and dielectric

properties. The numerical model simulation evaluated the TiO₂-film and the blood clot assembly, showing macroscopically a joint constant electrical conductivity (σ_{BC+TiO_2}). The value obtained in this study is in agreement with the expected values for analytical approaches. Previous studies have reported an electrical conductivity of the titanium oxide (TiO₂ film) formed on the dental implant surfaces within a thickness of 1-10 nm^{41,42} at 10⁻⁶ S/m⁴³ while the blood within a thickness of 0.45 mm³⁴ showed electrical conductivity at 0.6 S/m^{44,45}. However, several studies have shown that the electrical conductivity of TiO₂-film depends on the applied electric field^{33,46}. Also, computational simulation considering only blood (0.6 S/m⁴⁰) at the implant-bone interface could not reveal representative results as experimentally obtained from *in vivo* or electrochemical *in vitro* studies. Regarding the TiO₂-film changes on different environmental conditions, both the oxide thickness and the TiO₂ conductivity (between 10⁻⁷⁴⁷ and 10⁶ S/m⁴⁸) also vary during the blood coagulation process. Thus, the blood between the implant and the bone undergoes a coagulation process due to the reaction between fibrinogen and thrombin^{49,50}. That provides a decrease in electrical conductivity of one-fold after the coagulation process⁴⁹. The estimation of the electrical conductivity at the BIC region varies once the coagulation process depends on several factors such as temperature, implant surface, implant-to-bone micro-gap, blood sedimentation, and hematocrit⁵¹. The evaluation of the electrical and geometric properties of TiO₂-film and blood clot is a limitation of computation simulation.

The balanced electrical stimuli on titanium implants has some advantages regarding the cell migration, angiogenesis, and bone growth. The fundamentals on the electrical stimuli are related to the electrochemical reactions around the implant. On the direct

electrical stimuli, the titanium implant becomes a cathode while the bone and the surrounding tissues are the anode. Then, the electrical current flows around the implants through the surrounding medium leading to the formation of hydroxyl radical that increase the pH²⁷. As a result, the low oxygen content and the alkaline environment stimulate the activity of osteogenic cells and therefore the hydrogen peroxide content stimulates the release of vascular endothelial growth factors (VEGF)²². The continuous electrical stimuli at a well-controlled magnitude can regulate the osteoinductive growth factors, such as bone morphogenetic proteins (BMP-2, -6, and -7), which stimulates the cellular proliferation, differentiation, and extracellular matrix synthesis⁵⁵. That can enhance the bone growth by contact and distance osteogenesis processes within a bone healing speed-up⁵⁵.

In the present study, the finite element modeling and analysis considered the healing cap surrounded by the soft tissue (Figure 2A). Such information is relevant since the exposure of the healing cap can changes the conductivity of the implant. Thus, the degradation of the implant surface could affect the osseointegration process due to the release of corrosion products and Ti ions²⁴. Also, the change in pH due to peri-implant inflammatory reactions can affect the dielectric properties of the TiO₂-film according to the equation in Figure 2B. In fact, the soft tissue shields the wound against injuries, acidic substances, and bacteria-induced infections from the oral cavity. After that, an abutment will replace the healing cap to promote the establishment of the anatomical features of the peri-implant soft tissues.

The materials involved in the chemical composition of the implant, abutment, and battery determine the electrical resistance of the implant surface and electrical current

flow at the peri-implant region, as illustrated in Figure 1 and 2. That change becomes significant in the case of $\sigma_{\text{BC+TiO}_2} \leq 0.1 \text{ S/m}$, $I_T \leq 17.12 \mu\text{A}$. In that case, there was a decrease of around 18% in electrical current source. However, such decrease in electrical source was not enough to affect osseointegration stimulation as seen in Figure 4. The current density distribution (J) through the implant on $\sigma_{\text{BC+TiO}_2} = 0.3 \text{ S/m}$, considering high conductivity values generate a low resistance value, as shown in Figure 5. At the peak of the implant screw thread, bone-implant interface revealed slightly better results (rainbow color) when compared to the valley region (current density distribution below 0.15 A/m^2). That indicated an influence of the implant macro-geometry on the current density distribution at different regions of the implant. An issue that remains unclear deals with optimal electrical stimulation, related to both electric current density and intensity considering the individual variation in bone density. Nevertheless, experimental studies in literature have not followed any standard requirement, leading to bias in comparing results or to draw conclusions for suitable application in human bone healing. Common parameters applied include DC current at around $1\text{-}50 \mu\text{A/cm}^2$, which can affect osteoblast proliferation and gene expression of cell differentiation^{24,27,28}. Previous studies also reported different direct current amplitudes, ranging from 7 to up $50 \mu\text{A}$ ²⁵, to induce bone formation. Some studies reported an enhancement of bone healing in tibiae and femurs of rabbits or dogs after electrical stimulation at $10\text{-}20 \mu\text{A}$ over different periods of time^{52,53}.

The numerical model was also capable to demonstrate the highest BIC percentage when applying electric current from 30 and $40 \mu\text{A}$ ($\sim 90\%$), as seen in Figure 6. The results of the present work also indicated that an applied electric current above $40 \mu\text{A}$ can exhibit an electrical current density higher than 0.5 A/m^2 , which may cause tissue

damage²⁴. The mathematical model used in our study showed that the application of the optimum current source position at 20 μA was at the apical peri-implant region ($h=10\text{ mm}$), resulting in 86.1% of the BIC area (Fig. 6). In this way, a decrease in BIC percentage of around 10% was recorded when the electrical stimuli source was placed at the cervical peri-implant region (peri-implant bone crest) (Fig. 7). Although 75.4% of the BIC area has acceptable current density for osseointegration, such electrical distribution was heterogeneous, showing $I < 0.01\text{ A/m}^2$ at the apical peri-implant region.

Considering the previous findings, Bins-Ely et al.²³ showed that the increase in BIC area was higher when electrical stimuli were applied, as evidenced by statistically significant differences between the test (10 μA and 20 μA) and control (0 μA) groups over a period of 15 days ($p < 0.01$). Narkhede⁵⁴ demonstrated in a study in rabbit that an electrical stimulus at 20 μA did not affect the bone formation around implant. The highest BIC results were obtained in animals undergoing 40 μA stimulus over periods of 35 and 50 days. Long-term periods of electrical stimulation on 100 μA were detrimental to the process of bone formation⁵⁴. A more recent study in rabbit, conducted by Fredericks et al⁵⁵ suggested that DC stimulation at 100 μA , during 4 weeks, increase the rate and extent of bone formation for 4 weeks due to the up-regulation of osteoinductive factors. Corroborating with this finding, Brighton et al⁵³ reported electrochemically reduction in oxygen tension and a considerable elevation in pH occurred at 100 μA , known to cause necrosis in vivo. Also, another previous study reported a risk of osteolysis on electrical current above 30 μA ⁵⁶.

In despite of the current flow is not uniform along the surrounding bone–implant

interface ²³, previous studies have also reported bone formation after electrical stimulation associated with dental implants placed in dog mandible ^{30,57,58}. Therefore, the positioning of the electric current source inside implant (cervical *versus* apical peri-implant regions) and implant design, could change the BIC area rates. In the present study, finite element analysis (FEA) reveals significant information on the flow path and intensity of the electrical current around the titanium implant to bone region. Thus, the electrical current flow occurs through the path at low electrical resistance between the implant and the surrounding bone. As a result, some regions can have a higher current density than other regions as shown in the present findings. The cell stimulation and bone growth are higher in the peri-implant region on balanced current stimuli. Several parameters related to the implant design, materials, and bone type should be further studied by FEA in association with positioning and type of the electrical source.

5. Conclusions

Within the limitations of a mathematical model of a previous *in vivo* study, the main outcomes of this work can be summarized as follow:

- Electrical current source below 10 μA might not provide a required resultant current density for osseointegration as indicated by bone-implant contact percentage less than 55%. However, electrical current sources ranging from 10 up to 20 μA could increase the bone-implant contact up to about 60% while source ranging from 30 up to 40 μA can result in bone-implant contact percentage at around 90%;
- Regarding the positioning of the electrical source, the application of the

electrical current source at the apical peri-implant region (closer to the implant apex) resulted in 86.1% bone-implant contact. The electrical current source at the coronal region might decrease the bone-implant percentage;

- The macrogeometry of the implant thread region might play a crucial role on the current density at the bone-implant interface. Also, the exposure of the healing cap would change the electrical conductivity of the implant and electrical current flow at the peri-implant region. Further studies should consider such parameters to clarify the electrical current flow at the bone surrounding the implant.

Acknowledgments

This work was financed by the Conselho Nacional de Desenvolvimento Científico e Tecnológico (CNPq) the PVE/CAPES/CNPq 407035/2013-3.

References

1. Brånemark PI, Hansson BO, Adell R, Breine U, Lindström J, Hallén O OA. Osseointegrated implants in the treatment of the edentulous jaw. Experience from a 10-year period. *Scand J Plast Reconstr Surg Suppl* 1977;**16**:1–132.
2. Esposito M., Murray-Curtis L., Grusovin MG., Coulthard P., Worthington H V. Interventions for replacing missing teeth: different types of dental implants. *Cochrane Database Syst Rev* 2007;(7). Doi: 10.1002/14651858.CD003815.pub3.
3. Puleo DA., Nanci A. Understanding and controlling the bone- implant interface. *Biomaterials* 1999;**20**(23–24):2311-21.

4. van Velzen FJJ., Ofec R., Schulten EAJM., ten Bruggenkate CM. 10-year survival rate and the incidence of peri-implant disease of 374 titanium dental implants with a SLA surface: A prospective cohort study in 177 fully and partially edentulous patients. *Clin Oral Implants Res* 2015. Doi: 10.1111/clr.12499.
5. Albrektsson T., Wennerberg A. Oral implant surfaces: Part 2 - review focusing on clinical knowledge of different surfaces. *Int J Prosthodont* 2004;**17**(5):544–64. Doi: 10.1098/rsta.2009.0062.
6. Pourdanesh F., Esmaeelinejad M., Aghdashi F. Clinical outcomes of dental implants after use of tenting for bony augmentation: a systematic review. *Br J Oral Maxillofac Surg* 2017. Doi: 10.1016/j.bjoms.2017.10.015.
7. Schiegnitz E., Al-Nawas B. *Bilal Al-Nawas, Prof Dr Dr Augmentation procedures using bone substitute materials or autogenous bone-a systematic review and meta-analysis*. n.d.
8. Coelho PG., Granjeiro JM., Romanos GE., Suzuki M., Silva NRF., Cardaropoli G., et al. Basic research methods and current trends of dental implant surfaces. *J Biomed Mater Res - Part B Appl Biomater* 2009. Doi: 10.1002/jbm.b.31264.
9. Negri B., Calvo-Guirado JL., Maté Sánchez de Val JE., Delgado Ruiz RA., Ramírez Fernández MP., Gómez Moreno G., et al. Biomechanical and Bone Histomorphological Evaluation of Two Surfaces on Tapered and Cylindrical Root Form Implants: An Experimental Study in Dogs. *Clin Implant Dent Relat Res* 2013. Doi: 10.1111/j.1708-8208.2011.00431.x.
10. ALFARSI MA., HAMLET SM., IVANOVSKI S. Titanium surface hydrophilicity enhances platelet activation. *Dent Mater J* 2014. Doi: 10.4012/dmj.2013-221.
11. Himmlova L., Kubies D., Hulejova H., Bartova J., Riedel T., Stikarova J., et al.

- Effect of Blood Component Coatings of Enosseal Implants on Proliferation and Synthetic Activity of Human Osteoblasts and Cytokine Production of Peripheral Blood Mononuclear Cells. *Mediators Inflamm* 2016. Doi: 10.1155/2016/8769347.
12. Davies J. Understanding peri-implant endosseous healing. *J Dent Educ* 2003;**67**(8):932–49.
 13. Salou L., Hoornaert A., Louarn G., Layrolle P. Enhanced osseointegration of titanium implants with nanostructured surfaces: An experimental study in rabbits. *Acta Biomater* 2015. Doi: 10.1016/j.actbio.2014.10.017.
 14. Bosshardt DD., Chappuis V., Buser D. Osseointegration of titanium, titanium alloy and zirconia dental implants: current knowledge and open questions. *Periodontol 2000* 2017;**73**(1):22–40. Doi: 10.1111/prd.12179.
 15. Kopf BS., Ruch S., Berner S., Spencer ND., Maniura-Weber K. The role of nanostructures and hydrophilicity in osseointegration: In-vitro protein-adsorption and blood-interaction studies. *J Biomed Mater Res - Part A* 2015. Doi: 10.1002/jbm.a.35401.
 16. Cochran D., Oates T., Morton D., Jones A., Buser D., Peters F. Clinical Field Trial Examining an Implant With a Sand-Blasted, Acid-Etched Surface. *J Periodontol* 2007;**78**(6):974–82. Doi: 10.1902/jop.2007.060294.
 17. Rocuzzo M., Aglietta M., Bunino M., Bonino L. Early loading of sandblasted and acid-etched implants: A randomized-controlled double-blind split-mouth study. Five-year results. *Clin Oral Implants Res* 2008;**19**(2):148–52. Doi: 10.1111/j.1600-0501.2007.01426.x.
 18. Bornstein MM., Lussi A., Schmid B., Belser UC., Buser D. Early loading of

- nonsubmerged titanium implants with a sandblasted and acid-etched (SLA) surface: 3-year results of a prospective study in partially edentulous patients. *Int J Oral Maxillofac Implants* 2003;**18**:659–66. Doi: 10.1111/j.1600-0501.2005.01209.x.
19. Nevins M., Parma-Benfenati S., Quinti F., Galletti P., Sava C., Sava C., et al. Clinical and Histologic Evaluations of SLA Dental Implants. *Int J Periodontics Restorative Dent* 2017;**37**(2):175–81. Doi: 10.11607/prd.3131.
 20. Le Guéhennec L., Soueidan A., Layrolle P., Amouriq Y. Surface treatments of titanium dental implants for rapid osseointegration. *Dent Mater* 2007:844–54. Doi: 10.1016/j.dental.2006.06.025.
 21. Ribeiro AR., Oliveira F., Boldrini LC., Leite PE., Falagan-Lotsch P., Linhares ABR., et al. Micro-arc oxidation as a tool to develop multifunctional calcium-rich surfaces for dental implant applications. *Mater Sci Eng C Mater Biol Appl* 2015;**54**:196–206. Doi: 10.1016/j.msec.2015.05.012.
 22. Song JK., Cho TH., Pan H., Song YM., Kim IS., Lee TH., et al. An electronic device for accelerating bone formation in tissues surrounding a dental implant. *Bioelectromagnetics* 2009. Doi: 10.1002/bem.20482.
 23. Bins-Ely LM., Cordero EB., Souza JCM., Teughels W., Benfatti CAM., Magini RS. In vivo electrical application on titanium implants stimulating bone formation. *J Periodontal Res* 2017;**52**(3). Doi: 10.1111/jre.12413.
 24. Gittens RA., Olivares-Navarrete R., Tannenbaum R., Boyan BD., Schwartz Z. Electrical implications of corrosion for osseointegration of titanium implants. *J Dent Res* 2011;**90**(12):1389–97. Doi: 10.1177/0022034511408428.
 25. Nelson FRT., Brighton CT., Ryaby J., Simon BJ., Nielson JH., Lorch DG., et al. Use

- of physical forces in bone healing. *J Am Acad Orthop Surg* 2003. Doi: 10.5435/00124635-200309000-00007.
26. Cochran BVG. EXPERIMENTAL METHODS FOR STIMULATION OF BONE HEALING BY MEANS OF ELECTRICAL ENERGY* The concept of stimulating the formation of bone electrically is suggested by the presence of physiologic electric currents in living bone. These currents are thought to r. *Bull N Y Acad Med* 1972;**48**(7):899–911.
 27. Bodamyali T., Kanczler J., Simon B., Blake D., Stevens C. Effect of Faradic Products on Direct Current-Stimulated Calvarial Organ Culture Calcium Levels. *Biochem Biophys Res Commun* 1999;**264**:657–61.
 28. Kim IS., Song JK., Zhang YL., Lee TH., Cho TH., Song YM., et al. Biphasic electric current stimulates proliferation and induces VEGF production in osteoblasts. *Biochim Biophys Acta - Mol Cell Res* 2006. Doi: 10.1016/j.bbamcr.2006.06.007.
 29. Matsumoto H., Ochi M., Abiko Y., Hirose Y., Kaku T., Sakaguchi K. Pulsed electromagnetic fields promote bone formation around dental implants inserted into the femur of rabbits. *Clin Oral Implants Res* 2000. Doi: 10.1034/j.1600-0501.2000.011004354.x.
 30. Shayesteh YS., Eslami B., Dehghan MM., Vaziri H., Alikhassi M., Mangoli A., et al. The effect of a constant electrical field on osseointegration after immediate implantation in dog mandibles: A preliminary study: Basic science research. *J Prosthodont* 2007. Doi: 10.1111/j.1532-849X.2007.00208.x.
 31. Wang J., Tang N., Xiao Q., Zhang L., Li Y., Li J., et al. Pulsed electromagnetic field may accelerate in vitro endochondral ossification. *Bioelectromagnetics* 2015. Doi: 10.1002/bem.21882.

32. Barak S., Neuman M., Iezzi G., Piattelli A., Perrotti V., Gabet Y. A new device for improving dental implants anchorage: A histological and micro-computed tomography study in the rabbit. *Clin Oral Implants Res* 2015. Doi: 10.1111/clr.12661.
33. Diebold U. The surface science of titanium dioxide. *Surf Sci Rep* 2003. Doi: 10.1016/S0167-5729(02)00100-0.
34. Vanegas-Acosta JC., Landinez P. NS., Garzón-Alvarado DA. Mathematical model of the coagulation in the bone-dental implant interface. *Comput Biol Med* 2010. Doi: 10.1016/j.combiomed.2010.08.002.
35. Raj Vankayala R., Petrick Lai W-J., Cheng K-C., Chu Hwang K. Enhanced electrical conductivity of nylon 6 composite using polyaniline-coated multi-walled carbon nanotubes as additives. *Polymer (Guildf)* 2011;52:3337–43. Doi: 10.1016/j.polymer.2011.05.007.
36. Li T., Hu K., Cheng L., Ding Y., Ding Y., Shao J., et al. Optimum selection of the dental implant diameter and length in the posterior mandible with poor bone quality - A 3D finite element analysis. *Appl Math Model* 2011. Doi: 10.1016/j.apm.2010.07.008.
37. Kim HJ., Yun HS., Park H Do., Kim DH., Park YC. Soft-tissue and cortical-bone thickness at orthodontic implant sites. *Am J Orthod Dentofac Orthop* 2006. Doi: 10.1016/j.ajodo.2004.12.024.
38. Motoyoshi M., Yoshida T., Ono A., Shimizu N. *Effect of Cortical Bone Thickness and Implant Placement Torque on Stability of Orthodontic Mini-implants*. 2007.
39. Sadiku MNO. *Elements of Electromagnetics*. 6th ed. 2014.
40. Gabriel S., Lau RW., Gabriel C. The dielectric properties of biological tissues: III.

- Parametric models for the dielectric spectrum of tissues. *Phys Med Biol* 1996;**41**(11):2271.
41. Guo CY., Matinlinna JP., Tang ATH. Effects of surface charges on dental implants: Past, present, and future. *Int J Biomater* 2012. Doi: 10.1155/2012/381535.
 42. Gittens RA., Olivares-Navarrete R., Rettew R., Butera RJ., Alamgir FM., Boyan BD., et al. Electrical polarization of titanium surfaces for the enhancement of osteoblast differentiation. *Bioelectromagnetics* 2013. Doi: 10.1002/bem.21810.
 43. Pan, J., Thierry D., Leygraf C. *Hydrogen peroxide toward enhanced oxide growth on titanium in PBS solution: Blue coloration and clinical relevance*. n.d.
 44. Peratta C., Peratta A. *Modelling the human body exposure to ELF electric fields*. UK; 2010.
 45. Gabriel C., Gabriel S., Corthout E. *The dielectric properties of biological tissues: I. Literature survey*. vol. 41. 1996.
 46. Jankowski B. Preparation and electrical properties of Ti-TiO₂-Metal thin film structures. *Thin Solid Films* 1976. Doi: 10.1016/0040-6090(76)90130-9.
 47. Regonini D., Adamaki V., Bowen CR., Pennock SR., Taylor J., Dent ACE. AC electrical properties of TiO₂ and Magnéli phases, Ti_nO_{2n-1}. *Solid State Ionics* 2012;**229**:38–44. Doi: 10.1016/j.ssi.2012.10.003.
 48. Donachie MJ. *Titanium: a technical guide*. ASM international; 2000.
 49. Ur A. *Detection of Clot Retraction Through Changes of the Electrical Impedance of Blood during Coagulation*. n.d.
 50. Lei KF., Chen KH., Tsui PH., Tsang NM. Real-Time Electrical Impedimetric Monitoring of Blood Coagulation Process under Temperature and Hematocrit Variations Conducted in a Microfluidic Chip. *PLoS One* 2013. Doi:

- 10.1371/journal.pone.0076243.
51. Ramaswamy B., Yeh YTT., Zheng SY. Microfluidic device and system for point-of-care blood coagulation measurement based on electrical impedance sensing. *Sensors Actuators, B Chem* 2013. Doi: 10.1016/j.snb.2011.11.031.
 52. Friedenber g Z., Andrews E., Smolenski B., Pearl B., Brighton CT. Bone reaction to varying amounts of direct current. *Surg Gynecol Obs* 1970;**131**(5):894–9.
 53. Brighton C., Friedenber g Z., Zemsky LM., Pollis P. Direct-current stimulation of non-union and congenital pseudarthrosis. Exploration of its clinica application. I. *J Bone Jt Surg* 1975;**57**(3):368–77.
 54. Narkhede PR. *A HISTOLOGIC EVALUATION OF THE EFFECT OF ELECTRICAL STIMULATION ON OSTEOGENIC CHANGES FOLLOWING PLACEMENT OF BLADE-VENT IMPLANTS IN THE MANDIBLE OF RABBITS*. vol. 185. n.d.
 55. Fredericks DC., Smucker J., Petersen EB., Bobst JA., Gan JC., Simon BJ., et al. Effects of direct current electrical stimulation on gene expression of osteopromotive factors in a posterolateral spinal fusion model. *Spine (Phila Pa 1976)* 2007. Doi: 10.1097/01.brs.0000251363.77027.49.
 56. Friedenber g Z., Zemsky L., Pollis R. The Response of Non-Traumatized Bone to Direct Current. *JBJS* 1974;**56**(5):1023–30.
 57. Shigino., Ochi., Kagami., Sakaguchi., Nakade. Application of Capacitivel y Coupled Electric Field Enhances Periimplant Osteogenesis in the Dog Mandible. *Nt J Prosthodont* 2000;**13**(5):365–372.
 58. Shigino T., Ochi M., Hirose Y., Hirayama H., Sakaguchi K. *Enhancing Osseointegration by Capacitively Coupled Electric Field: A Pilot Study on Early Occlusal Loading in the Dog Mandible*. 2001.

